Asian Journal of Chemistry; Vol. 23, No. 11 (2011), 5025-5030

ASIAN JOURNAL OF CHEMISTRY

www.asianjournalofchemistry.co.in

Nanoparticles of Dibromo-*p*-sulfonic Acid-Arsenazo Encapsulated in SBA-15

QING-ZHOU ZHAI*, SHUN HU, XIAO-DONG LI and HUI YU

Research Center for Nanotechnology, Changchun University of Science and Technology, 7186 Weixing Road, Changchun 130022, P.R. China

*Corresponding author: Fax: +86 431 85383815; Tel: +86 431 85583118; E-mail: zhaiqingzhou@163.com; zhaiqingzhou@hotmail.com

(*Received*: 19 January 2011; *Accepted*: 25 July 2011) AJC-10203

DBS-Arsenazo (dibromo-*p*-sulfonic acid arsenazo, DBS-ASA) nanoparticles were prepared within sileceous SBA-15 mesoporous molecular sieve by liquid method. A series of characterizations including chemical analysis, infrared spectra, powder X-ray diffraction analysis, scanning electron microscopic study, nitrogen adsorption-desorption study, photoluminescence study were used to characterize the host-guest (SBA-15)-(DBS-ASA) nanocomposite compounds. Nitrogen adsorption-desorption study, chemical analysis revealed that DBS-ASA incorporated into the host SBA-15. Nitrogen adsorption measurements revealed mesoporosity for the host-guest nanocomposite materials accompanied by a reduction of the surface area and pore volume, both indications of a decoration of the inner surface of the molecular sieve walls. IR and XRD investigations showed that the mesoporous host structure was still kept in the host-guest composite compounds. XRD measurements proved that the existence of disordered DBS-ASA nanoparticles. SEM investigations showed that the shape of (SBA-15)-(DBS-ASA) was claviform and the size of (SBA-15)-(DBS-ASA) was 328 ± 10 nm. The nonacomposite materials (SBA-15)-(DBS-ASA) have a property of luminescence at 470 nm and may become a promising luminescent material.

Key Words: SBA-15 molecular sieve, Dibromo-*p*-sulfonic acid arsenazo, Host-guest nanocomposite material, Luminous material.

INTRODUCTION

Since the researchers of American Mobil Corporation firstly reported a kind of pore channel arrangement high ordered property mesoporous molecular sieve materials in 1992, mesoporous compunds and their related composite materials have become the research field. Among them, mesoporous molecular sieves are used as hosts to incorporate other materials on the nanoscale to form nanocomposite materials, which have potential applied value in the fields of solid lasers, full colour vision, sun energy cell sensing part, *etc*.[1-5]. Since SBA-15 was synthesized[6], it is gradually concerned by several researchers[7-16]. It has the following characteristics *i.e.*, the synthesis method is simple, the pore channels present hexaganol highly ordered, specific surface area is large, pore size distribution is very narrow,surface chemical properties are rich, *etc*. Compared with other molecualr sieves, SBA-15 has the characteristics that pore channels are homogeneously controlled, highly ordered, pore size is large (5-30 nm) and its hydrothermal stability is excellent, *etc*. These special properties made SBA-15 have tremendous applied foreground in many fileds such as separation, catalysis, biology and nanomaterials, *etc*. As SBA-15 molecualr sieve has big and ideal periodic arrangement nanopore channels, which made it ideal hosts for producing quantum dots, quantum wires nanostructures, *etc*. In recent years,in the aspect of incorporating protein it caused scientists' enormous interests[17,18]. Some dyes such as malachite green have been incorporated into MCM-41 molecular sieves[19]. Dibromo-*p*-sulfonic acid arsenazo[DBS-arsenazo, 3-(2,6-dibromo-4-sulfophenylazo)-6-(2-arseno-phenylazo)-4,5-dihydroxynaphthalene-2,7-disulfonic acid, abbreviated as DBS-ASA] is an azo dye reagent[20]. To our best of knowledge, the study where SBA-15 is used as host and DBS-ASA is incorporated into it has not reported earlier. The present study uses SBA-15 as host and using liquid method DBS-arsenazo is incorporated into SBA-15 channels to prepare (SBA-15)-(DBS-ASA) nanocomposite materails. Chemical analysis, infrared spectra, powder X-ray diffraction, scanning electron microscopy, low temperature nitrogen adsorption-desorption at 77 K, photoluminescence study were employed to characterize the prepared nanocom-posite materials with good results.

EXPERIMENTAL

Tricopolymerpoly(ethylene glycol)-block-poly(propyl glycol)-block-poly(ethylene glycol) ($EG_{20}PG_{40}EG_{20}$, average molecular weight 5800, Aldrich); tetraethyl orthosilicate (TEOS, 98 %, Fluka); 2 mol/L of hydrochloric acid solution (AR, Changchun Chemical Leechdom Corporation, Ltd., China); Trimethylchlorosilane (AR, Shanghai Chemical

Corporation of Chinese Medicine Group, China); dibromo-*p*-sulfonic acid arsenazo ($C_{22}H_{15}AsBr_2N_4O_{14}S_3$, East China Normal University, Shanghai, China). The water used in the experiments was deionized water whose electric conductivity was 0.08 μS/cm.

Preparation of SBA-15 host material: Mesoporous silica SBA-15 was synthesized according to reported procedure[6]. In the acidic condition, the triblock copolymer, $EG_{20}PG_{40}EG_{20}$ was used as the structure-directing template and TEOS was used as silica source. In a typical synthesis, 2 g of the template was dissolved in 60 g of 2 mol/L hydrochloric acid and 15 g of deionized water with stirring, then 4.25 g of TEOS was added, stirred for 24 h at 40 ºC. The mixture was placed in a Teflon-liner autoclave treated at 100 ºC for 48 h. After crystallization, the product was filtered and washed with deionized water and dried at room temperature.

The outside surface of the SBA-15 molecular sieve was modified by trimethylchlorosilane before calcination. After the reaction, the silanol groups of the SBA-15 surface were replaced by CH_3-group of trimethylchlorosilane. Then, the sample was calcined at temperature 550 ºC for 24 h. The purpose was to eliminate the template and the silane was oxidized off from the outside surface of the SBA-15. In this work, for the modification of the SBA-15 with silane prior calcination, it is expected that all of the silane can be oxidized off from the outside surface of the SBA-15, but the silanol groups of the inner surface of the pore channels can be kept as such. The purpose was DBS-ASA is grafted on the inner surface of the pore channels of the SBA-15 but not grafted on the outside surface of the SBA-15.

The procedure for the preparation of modified SBA-15 material is as follows: 0.5 g of the uncalcined mesoporous SBA-15 powder was immersed in 15 mL of 1 % (v/v) trimethylchlorosilane in absolute ethanol solution and stirred for 24 h at room temperature. The solid product was filtered off, washed with absolute ethanol solution and dried at room temperature. The obtained material was calcined at temperature 550 ºC for 24 h and it was used as host material.

Preparation of (SBA-15)-(DBS-ASA) nanocomposite material: 0.200 g of the SBA-15 was placed in 20 mL of 1.0×10^{-3} mol/L DBS-arsenazo solution for the incorporation of the guest at room temperature for 48 h. The product was then filtrated and repeatedly washed using deionized water untill filtrate was colourless. The product was dried at 50 ºC for 5 h to obtain host-guest composite material.

Characterization methods: The content of silicon was determined by gravimetric method. Fourier transform infrared (FT-IR) spectra of the samples were collected with German BRUKER Vertex-70 spectrometer. XRD patterns were obtained on a D5005 diffractometer of German Siemens Company with CuK_α radiation. Scanning electron micrographs of the samples were recorded on a Japanese JEOL JSM-5600L to observe the morphology of the samples. Specific surface area, total pore volume and average pore diameter were measured by N_2 adsorption-desorption isotherms at 77 K using American Micromeritics ASAP2010M (Mike Company). The pore size was calculated on the adsorption branch of the isotherms using BJH (Barrett-Joyner-Halenda) method and the specific surface area was calculated using BET (Brunner-Emmett-Teller) method. The pore volume was taken at $P/P_0 = 0.974$ (single point). Room temperature (25 ºC) photoluminescence spectra were measured on an American PEX-FL-2T-2 (SPEX Company) spectrofluorophotometer.

RESULTS AND DISCUSSION

Chemical analysis: A content of SiO_2 in the sample (SBA-15)-(DBS-ASA) was determined by gravimetry and the SiO_2 determined in the (SBA-15)-(DBS-ASA) was 96.01 %. By difference method, the content of DBS-ASA obtained was 3.99 %.

Infrared spectra: FT-IR spectra of SBA-15, trimethylchlorosilane-modified SBA-15 (uncalcined) and trimethylchlorosilane-modified SBA-15 (calcined) are given in Fig. 1. From the spectra it can be seen that before calcination of trimethylchlorosilane-modified SBA-15 a band that appeared at 2965 cm^{-1} (curve C) is methyl C-H characteristic IR peak[21]. However, from curve B, the methyl C-H characteristic peak does not appear. This is because the methyl was wiped off from the outside surface of the SBA-15 under the condition of high temperature. The peak at 963 cm^{-1} is assigned to the stretching of silanol groups O-H of the SBA-15, the peak disappeared for the sample before calcination. It suggests that the methyl group has replaced the silanol group, but the peak appeared for the sample after calcination. It can be interpreted that the silanol groups of the inner surface of the pore channels have been well kept.

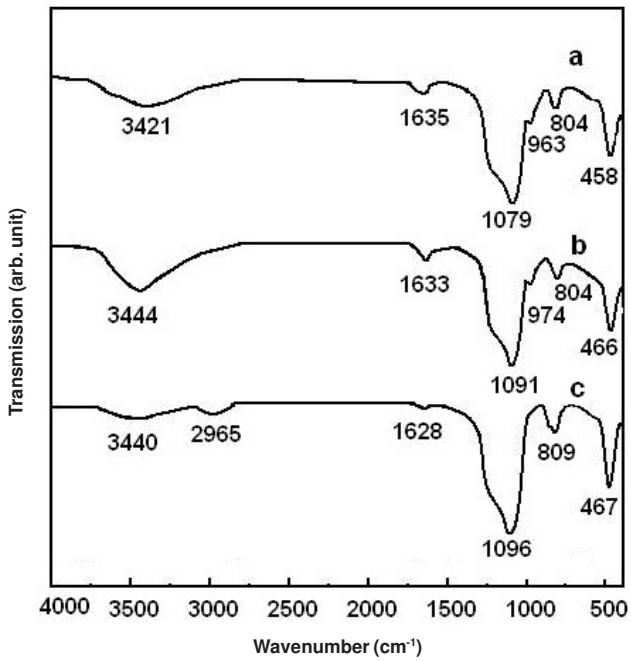

Fig. 1. Infrared spectra: (a) SBA-15; (b) post modification sample by chlorotrimethylsilane (calcined); (c) post modification sample by chlorotrimethylsilane (uncalcined)

The infrared spectra of SBA-15, DBS-ASA and (SBA-15)-(DBS-ASA) are given in Fig. 2. Compared with curve B with A and C, it is found that the infrared spectrum of (SBA-15)-(DBS-ASA) sample did not show the characteristic peak of DBS-ASA,showing that DBS-ASA uniformly dispersed

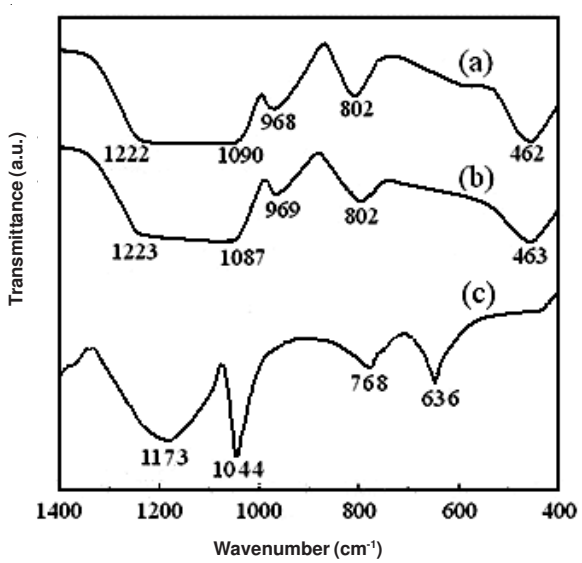

Fig. 2. Infrared spectra:(a) modified SBA-15; (b) (SBA-15)-(DBS-ASA); (c) DBS-ASA

in the channels of molecular sieve and no aggregated nanoscale crystal formed. The DBS-ASA existed in the form of quantum dots or quantum strings[21]. Host-guest nanocomposite material was formed by van der Waals forces between the host and guest.

Structure of mesoporous materials and scanning electron microscopic study: Powder X-ray diffraction is one of the main characterization methods for mesoporous materials of the SBA-15 and nanostructured host-guest composite materials, respectively. Powder X-ray diffraction patterns of SBA-15 and trimethylchlorosilane-modified SBA-15 samples in the range of 0.4-10º are shown in Fig. 3. They exhibit similar patterns with well-resolved diffraction peaks at 0.8º (2θ) and two weak peaks at 1.5 and 1.8º (2θ) due to (100), (110) and (200) Bragg reflections[6], respectively, showing that a good mesoscopic order and the characteristic hexagonal mesoporous structure of SBA-15 are maintained in trimethylchlorosilane-modified SBA-15 sample. The results also indicate that these materials have a good long-range order of mesostructure. Fig. 4 shows the wide-angle region over the range of 10-80º. As no distinguishable peak was found, the as-synthesized pure silica SBA-15 and trimethylchlorosilane-modified SBA-15 sample are amorphous.

The XRD pattern of (SBA-15)-(DBS-ASA) sample over the range of 0-10º is given in Fig. 5. From the figure it can be seen that the main characteristic diffraction peaks (100), (110), (200) of SBA-15 existed, revealing the SBA-15 molecular sieve framework in the composite materials prepared was well kept

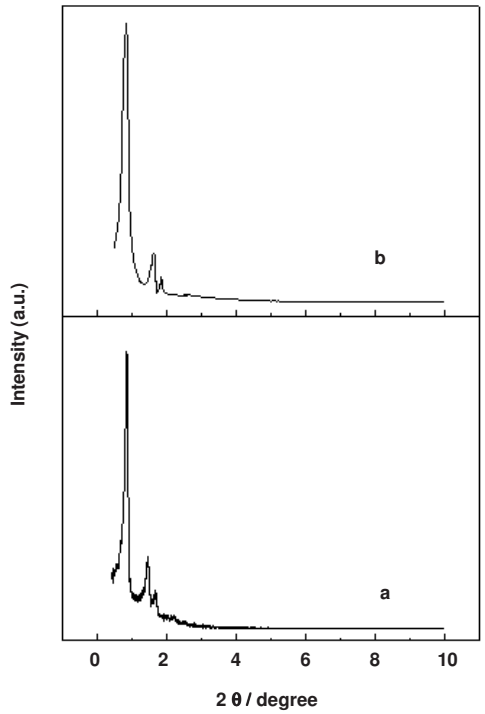

Fig. 3. Small angle XRD patterns of the samples:(a) SBA-15; (b) modified SBA-15

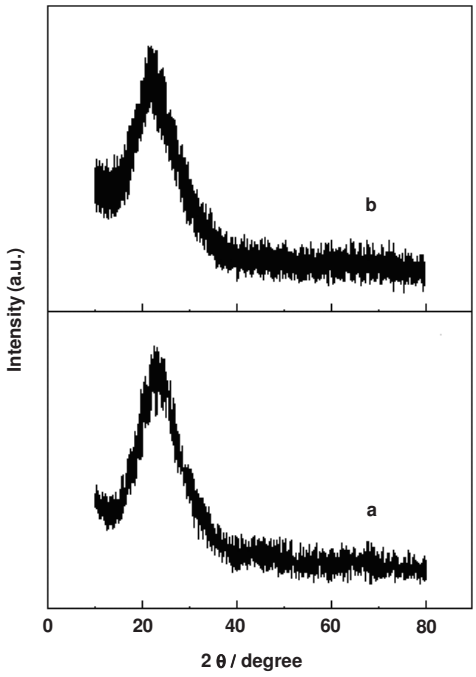

Fig. 4. Wide angle XRD patterns of the samples:(a) SBA-15; (b) modified SBA-15

TABLE-1
PORE STRUCTURE PARAMETERS OF THE SAMPLES

Sample	Crystal face spacing/d_{100} (nm)	Unit cell parameter/a_0 [a] (nm)	BET surface area (m^2/g)	Pore volume[b] (cm^3/g)	Pore size[c] (nm)	Wall thickness[d] (nm)	Content of DBS-ASA (wt. %)
Modified SBA-15	10.91	12.60	659	1.13	6.76	5.84	0
(SBA-15)-(DBS-ASA)	10.54	12.17	613	1.07	6.13	6.04	3.99

a: Unit cell parameter], $a_0 = \frac{2}{\sqrt{3}} d_{100}$. b: BJH adsorption cumulative volume of pore]. c: Pore size calculated from the adsorption branch. d: Wall thickness calculated by (a_0 – pore size).

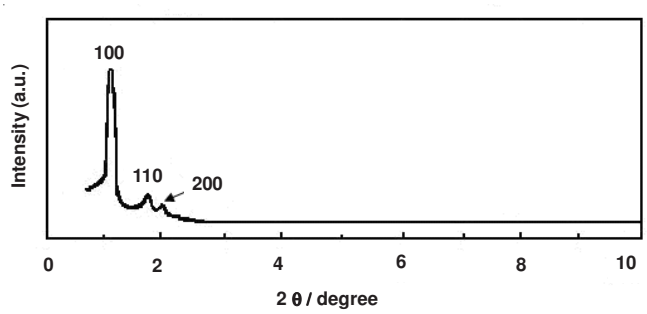

Fig. 5. Small angle XRD pattern of the sample (SBA-15)-(DBS-ASA)

and could successfully serve as nanotemplate of DBS-ASA. Fig. 6 is the wide-angle XRD diffraction pattern over the range of 10-80º. It can be seen that for the (SBA-15)-(DBS-ASA) sample no other characteristic peaks appeared, showing that the guest did not form aggregated nanocrystals in the host channels, but existed in the host channels in the form of quantum dots or quantum strings. The d(100) and cell parameters (a_0) obtained by calculation are listed in Table-1.

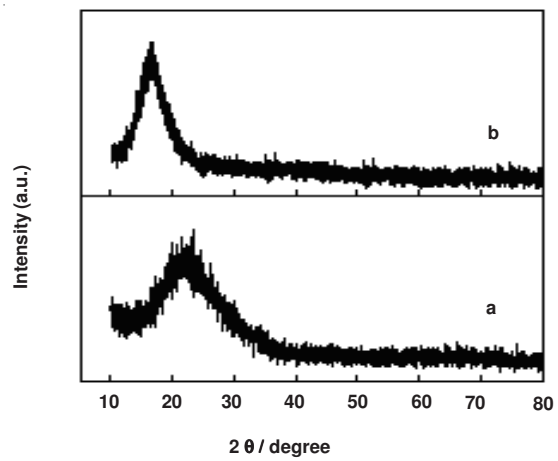

Fig. 6. Wide angle XRD patterns of the samples:(a) modified SBA-15; (b) (SBA-15)-(DBS-ASA)

The scanning electron microscopic images of the sample (SBA-15)- (DBS-ASA) is shown in Fig. 7. From the scanning microscopic images, the shape could be observed to be claviform and the average particle size was 328 ± 10 nm.

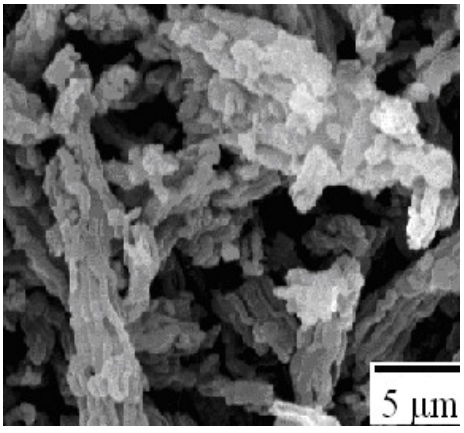

Fig. 7. SEM images of (SBA-15)-(DBS-ASA)

Porosity and surface area: Besides powder X-ray diffraction, nitrogen physisorption is the method of choice to characterize mesoporous materials. Physisorption gives information upon the specific surface area and the mean pore diameter. Nitrogen adsorption-desorption isotherms and pore size distribution patterns from the experiment carried out at 77 K to observe the textural changes in modified-SBA-15 molecular sieve and (SBA-15)-(DBS-ASA) nanocomposite materials are shown in Figs. 8 and 9, respectively. From the figures it can be seen that the adsorption isotherms of all materials SBA-15, (SBA-15)-(DBS-ASA) belong to typical Langmuir type IV (IUPAC classification)[21] with an H1 type hysteresis loop indicative of a typical feature of mesoporous materials and cylindrical pore shape. The sorption data have been used to get information about the mesoporosity, the total (BET) surface area, the total pore volume and also the pore diamensions according to BJH model. Under the condition of liquid nitrogen at 77 K, the adsorption process for nitrogen gas by single pore size distribution mesoporous material can be compartmentalized as the following phases:in low press phase, nitrogen molecules are adsorbed in the pore channels and thus adsorption curve is more smooth. When nitrogen molecules are adsorbed from monolayer to multilayer, adsorption curve rapidly breaks as pressure increases. When multilayer adsorption goes to capillary condensation, adsorption curve shows an obvious inflection point. When adsorption reaches saturation, an increase in adsorbed amount can also become slow as pressure increases. Over the middle pressure range the inflection point appeared results from quick capillary condensation and this is typical

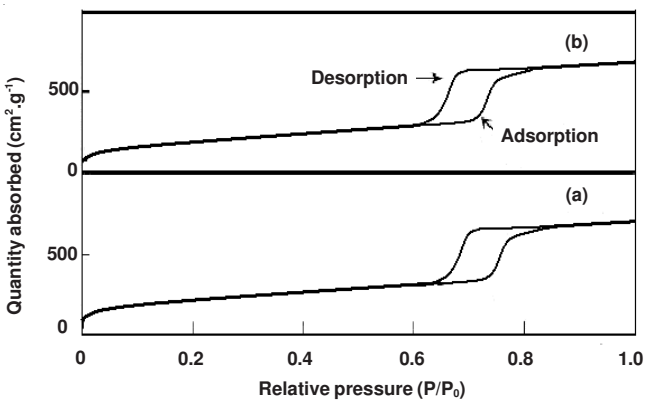

Fig. 8. Low temperature N_2 adsorption-desorption patterns of the samples: (a) modified SBA-15; (b) (SBA-15)-(DBS-ASA)

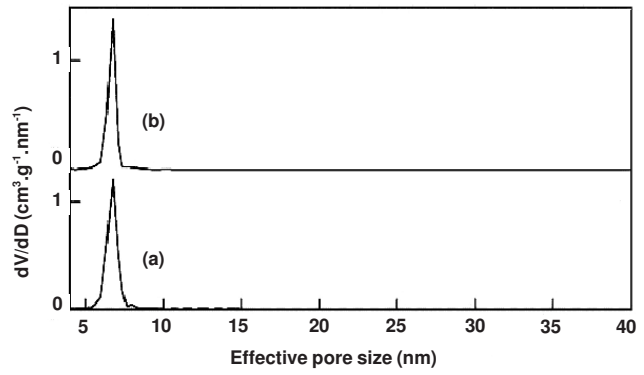

Fig. 9. Pore size distribution patterns of the samples: (a) modified SBA-15; (b) (SBA-15)-(DBS-ASA)

capillary condensation of mesoporous molecular sieve. However, capillary quick break is related to the pore size of mesoporous material. More pressure of break occured, more pore size of mesoporous molecular sieve. The N_2 adsorption-desorption curve shapes of (SBA-15)-(DBS-ASA) and modified-SBA-15 are similar and H1 type hysteresis loop in adsorption curve appeared in the adsorption curves, showing that the hexaganol phase mesoporous structure of SBA-15 did not change due to the introduction of DBS-arsenazo. When relative press was $P/P_0 < 0.62$ for the adsorption-desorption curve of modified-SBA-15, the adsorption curve shows gently increase. This is because nitrogen molecules were adsorbed inside the channels of mesoporous sieve in the form of single molecules and adsorption and desorption were reversible. When relative press was 0.62, adsorption curve had an obvious break and between adsorption and desorption curves an offset appeared. A obvious hysteresis loop appeared, which is due to that inside the mesoporous sieve of homogeneous pore chaneels capillary condensation phenomenon occurred. At this time, adsorption and desorption process was irreversible. When relative pressure $P/P_0 > 0.83$, the adsorbed amount of nitrogen gas reached saturation and adsorption curve tended to slow increase. Adsorption and desorption curves again renewedly coincided and capillary condensation phenomenon ended. Adsorption of nitrogen gas occurred between particles of the molecular sieve. For the adsorption-desorption curve of (SBA-15)-(DBS-ASA) nanocomposite material (curve B) the break took place at $P/P_0 = 0.59$,which is due to that incorporation of DBS-ASA into channels of SBA-15 resulted in a decrease in pore volume of the molecular sieve. Compared with those of SBA-15, the BET specific surface area, pore size and pore volume of (SBA-15)-(DBS-ASA) nanocomposite material decreased to some extent. This shows that DBS-ASA has been successfully encapsulated in the channels of mesoporous SBA-15 molecular sieve and partially occupied the channels of the molecular sieve. Fig. 8 is the pore size distribution curves of modified-SBA-15 and (SBA-15)-(DBS-ASA). They have size homogeneous one-dimensional cylindrical pore channel structure and pore size distribution was narrow. The (SBA-15)-(DBS-ASA) nanocomposite material still kept regular one-dimensional mesoporous character and at the same time the pore size distribution of (SBA-15)-(DBS-ASA) is narrower. Table-1 is the pore channel structure parameters of SBA-15 and (SBA-15)-(DBS-ASA).

Photoluminescence study: The excitation and emission spectra of the (SBA-15)-(DBS-ASA) sample is shown in Fig. 10. Semiconductor nanocrystals photoluminescence spectra generally consist of two light-emitting zones. A narrow and weak emission peak locates in a UV region, which comes from transitions between excitation energy levels of band edge, known as the band edge or excitation emission. The other is a wide and strong luminescence band located in a visible region, which is caused by transitions of impurities or defects, known as impurities or defects emission. In this work, the emission peak locates at 487 nm and in visible range and it is assigned to the defect luminescence. As the size of DBS-ASA was very small, the probability of forming defects on the surface is increased. Thus, the luminescence of the sample was caused

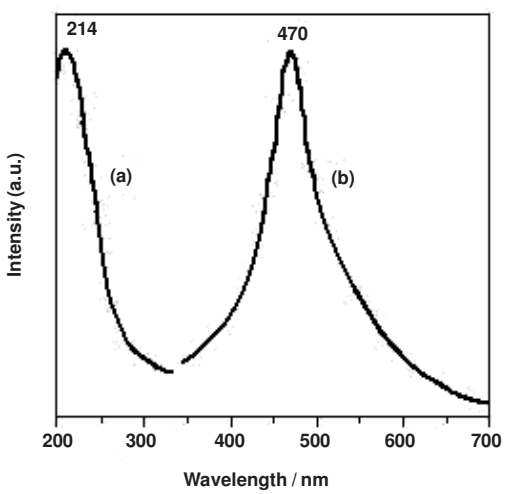

Fig. 10. Luminous spectrum of the (SBA-15)-(DBS-ASA) sample: (a) excitation spectrum;(b) emission spectrum

by surface defects. In solution, dye molecules agglomerate even under the condition of very small concentration. After agglomeration, the excitation energy of dye molecules is easy to release by thermal relaxation. Thus, the optically active performance is inhibited. The distance of dye molecules are far in mesoporous SBA-15 and their interaction is weaker. The contribution of fluorescence quenching is relatively small. Therefore, the material exhibits the luminescence properties similar to those of single molecules, showing strong luminous character. SBA-15 itself does not have the property of luminescence, but good luminous character appears after incorporating DBS-ASA. The (SBA-15)-(DBS-ASA) composite material prepared is expected to be applied as promising luminescence materials.

Conclusion

This study reports the characterization of nanoparticles of DBS-arsenazo encapsulated in SBA-15. Combined results of chemical analysis, IR, XRD, SEM and photoluminescence study have showed that DBS-arsenazo nanoparticles were encapsulated in the channels of SBA-15. The shape of (SBA-15)-(DBS-ASA) was claviform and the size of (SBA-15)-(DBS-ASA) was 328 ± 10 nm. The nanocomposite materials (SBA-15)-(DBS-ASA) have a property of luminescence at 470 nm and may become promising luminescent materials.

REFERENCES

1. Q.L. Zhao, J. Shen and X.D. Yuan, *Guangdong Chem. Ind*., **33**, 12 (2005).
2. S.J. Wu, J.H. Huang, T.H. Wu, K. Song, H.S. Wang, L.H. Xing, H.Y. Xu, L. Xu, J.Q. Guang and Q.B. Kan, *Chin. J. Catal*., **27**, 9 (2006).
3. J.Y. Qi, L.S. Qiang, M.S. Du, Y. Li and D.Y. Tand, *Rare Met. Mater. Eng*., **36**, 534 (2007).
4. C.L. Li, Y.Q. Wang and Y.L. Guo, *Chem. Mater*., **19**, 173 (2007).
5. W.P. Zhu, Y.C. Han and L.J. An, *Micropor.. Mesopor. Mater*., **80**, 221 (2005).
6. D.Y. Zhao, J.L. Feng, Q.S. Huo, N. Melosh, G.H. Fredrickson, B.F. Chmelka and G.D. Stucky, *Science*, **279**, 548 (1998).
7. C.W. Gu, P.A. Chia and X.S. Zhao, *Appl. Surf. Sci*., **237**, 387 (2004).
8. T. Asefa and R.B. Lennox, *Chem. Mater*., **17**, 2481 (2005).
9. L.H. Zhou, J. Hu, S.H. Xie and H.L. Liu, *Chin. J. Chem. Eng*., **15**, 507 (2007).
10. C.Z. Yao, X.R. Zhang, L.C. Wang, Y. Cao, W.L. Dai, K.N. Fan, D. Wu and Y.H. Sun, *Acta Chim. Sin.*, **64**, 269 (2006).

11. C.H. Tu, A.Q. Wang and M.Y. Zheng, *Chin. J. Catal*., **26**, 631 (2005).
12. L.H. Zhou, Y.Z. Xian, Y.Y. Zhou, J. Hu and H.L. Liu, *Acta Chim. Sin.*, **63**, 2117 (2005).
13. H. Song, R.M. Rioux, J.D. Hoefelmeyer, R. Komer, K. Niesz, M. Grass, P.D. Yang and G.A. Somorjai, *J. Am. Chem. Soc*., **128**, 3027 (2006).
14. N. Yuang, G. Cheng, D.K. Wang, Y.Q. An and Z.L. Du, *Acta Phys. Chim. Sin*., **25**, 2575 (2009).
15. B.H. Wu, S.C. Zhang, T. Tang, Y. Xu, Y. Liu and Z.H. Wu, *Acta Phys. Chim. Sin*., **26**, 2217 (2010).
16. S.C. Zhang, D. Jiang, T. Tang, J.H. Li and Y. Xu, *Acta Phys. Chim. Sin*., **26**, 1330 (2010).
17. M. Miyahara, A. Vinu and K. Ariga, *Mater. Sci. Eng*., **27C**, 232 (2007).
18. M. Hartmann, *Chem. Mater*., **17**, 4577 (2005).
19. X.D. Li, Q.Z. Zhai and M.Q. Zou, *Appl. Surf. Sci*., **257**, 1134 (2010).
20. J.M. Pan, Z.J. Li, Q.Y. Zhang and G.Z. Fang, New Chromogenic Reagents and their Application in Spectrophotometry, Beijing: Chemical Industry Press, p. 51 (2003).
21. H. Yu and Q.Z. Zhai, *Micropor. Mesopor. Mater*., **123**, 298 (2009).